Domain boundary engineering in (multi-) ferroics -concepts-

Ekhard Salje
University of Cambridge

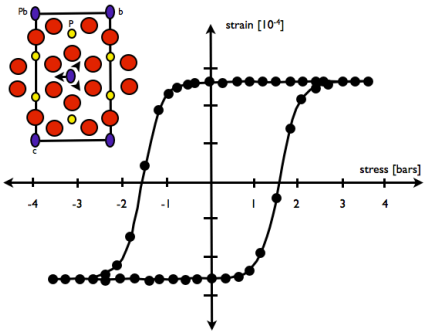

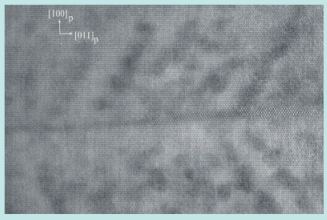

Typical wall thickness in perovskites at $T<<T_c$ is >2nm

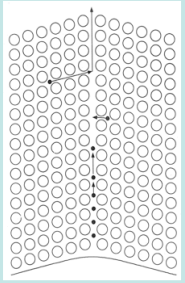

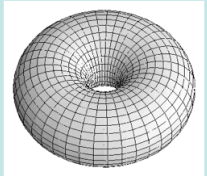

flexoelasticity: with a twin angle is 4° it would correspond to 90 segments in a torus with 2nm wall width and 60 nm diameter if all twin angles would be in the same direction with no domains in between (in fact they are zig-zag): all flexo-effects are hence hugh in twin walls (transport, band structure defomations, photovoltaics, multiferroics etc)!

The bulk: How to construct a Landau potential

Double well potential and order parameters

$L(Q, T, P) = 1/2\, A(\theta_t)(\coth \theta_t/T - \coth \theta_t/T_c)\, Q + 1/4\, BQ^4 + ...$

coupling ($-\varepsilon Q^2 - PQ^2 - MQ^2 ...$) leads to

$G(Q, T, P, \varepsilon, \pi, m, H_a, n, E, H)$

relaxation of G ($\partial G/\partial e = 0$, $\partial G/\partial \pi = 0$, $\partial G/\partial m = 0$) leads to and equilibrium G with field

$G(Q, T, P, H_a, n, E, H)$

and field - free $\sigma = E = H = 0$

$G(Q, T, P) = L^4(Q, T, P) + 1/2\, A^4(\theta_t(\coth \theta_t/T^4 - \coth \theta_t/T^4_c)\, Q + 1/4\, B^4Q^4 + ...$

DFT and other simulations can be put into the Landau framework: Landau theory is the playground where theory (of any kind) and experiment can meet.

Landau Ginzburg potential and the Euler-Lagrange equation

- Landau + dispersion term = Landau Ginzburg potent
- $G(Q) = 1/2AQ^2 + 1/4BQ^4 + 1/6CQ^6 + 1/2\, g\, (\text{grad}_x\, Q)^2$
- minimization: min G(Q) with boundary conditions,
- kink: $Q_o = 1$ for $x \rightarrow \infty$ and $Q_o = -1$ for $x \rightarrow -\infty$
- $\partial^2 Q/\partial r^2 = 1/g\, \{AQ + BQ^3 + CQ^6\}$
- most Euler-Lagrange equ. have NO analytical solution BUT for C=0 one finds the most important solution: $Q = Q_o \tanh (x/w)$ with $w = (2g/A)^{1/2}$
- numerical solutions can found easily, in pertubation theory on can write $Q = Q_o \tanh (x/w) + \varepsilon\, (Q)$

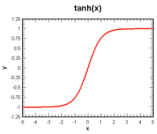

Ripple states

solution can become unstable so that higher order terms become necessary:
$+ 1/2\, d\, Q^2\, (\nabla Q)^2 + 1/2\, (\Delta Q)^2$

- trial function $\mathbf{Q = p + q \sin kx}$ **leading to**
  $\mathbf{G = Ap^2 + 1/2p^4 + 1/2Aq^2 + 3/2p^2q^2 + 3/16q^4 + (-\gamma/2q^2 + dp^2q^2 + d/4q^4)k^2 + 1/2q^2k^4}$
- **stable k vector : $k^2 = 1/2\gamma - d(p^2 + 1/4q^4) > 0$**
- $32G = -d^2q^6 + (6 + 47\gamma d)q^4 - (16 + 4\gamma^2)q^2 + 16p^4 + 32Ap^2 - 8d^2p^2q^2(2p^2 + q^2) + (48 + 16\gamma d)p^2q^2$.

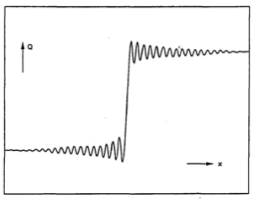

Ripple states near twin boundaries and surfaces

Mechanical model

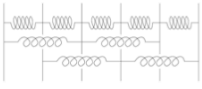

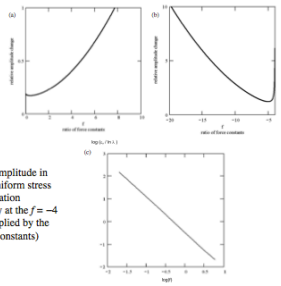

(a) Pressure dependence of the relative change of the relaxation amplitude in the 'anti-ferroelastic' regime ($\lambda > 0$). No singularity occurs for uniform stress fields. (b) Pressure dependence of the relative change of the relaxation amplitude in the 'ferroelastic' regime ($\lambda < 0$). Note the singularity at the $f = -4$ transition point. (c) Log/log plot of the precursor amplitude multiplied by the characteristic volume ($\log(\varepsilon\omega/\ln\lambda)$ versus the ratio of the force constants)

The two-spring model with free surfaces. Nearest neighbour layers are connected by a spring with force constant ϕ_1, the second nearest neighbours are connected by springs with the force constant ϕ_2 ($f = \phi_1/\phi_2$). The equilibrium distances are a_1 and a_2, the misfit parameter is $2a_1 - a_2$.

$H = \Sigma(\phi_1/2(b + \varepsilon_i - a_1)^2 + \phi_2/2(2b + \varepsilon_i + \varepsilon_{i+1} - a_2)^2)$
relaxation has a length scale: $\lambda = \pm 1/2(f^2 + 4f)^{1/2} - 1/2f - 1$

Salje EKH 2008 J.Phys. Cond. Matt. ***20*** 485003

wall orientation, analytical and by simulation

condition for strain walls to align along the 'easy' directions is that the strain tensors on both sides are rank 1 connected , explicitly for vanishing volume strain the compatibility relation:

$$[e_{ik}(S_1) - e_{ik}(S_2)]\, x_i x_k = 0$$

conditions for wall-bending is then that the compatibility=anisotropy energy $E_{anisotropy} = U(dy/dx)^2$ and the wall bending energy $E_{bending} = S(d^2y/dx^2)^2$ are minimised:

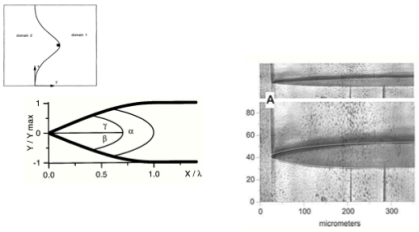

The hamiltonian

elastic forces are long-ranging:

ferro: $J(R) \sim (A_2Y_{2m} + A_4Y_{4m}) / R^3 + Jz$

antiferro: $J(R) \sim (A_2Y_{2m} + A_4Y_{4m} + A_6Y_{6m})/R^5$

bilinear coupling with the ordering scheme leads to a soft Ising model

$J_k \sim C_{\alpha\beta\gamma\lambda}\, e_{\alpha\beta}\, e_{\gamma\lambda} - P$ for $k=0$

$J_k \sim F_k^{\alpha}\, G_k^{\alpha\beta}\, F_k^{\beta} - P$ for $k \neq 0$

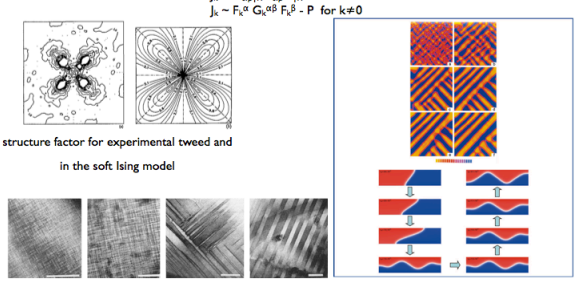

structure factor for experimental tweed and in the soft Ising model

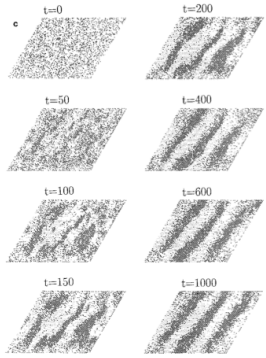

computer simulation of the annealing of a feldspar structure with Si/Al ordering after deep quench, note the 'easy' strain orientation.

ferrielectric twin walls in $CaTiO_3$

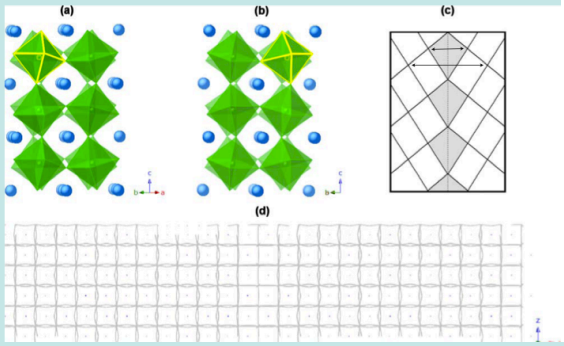

empirical potentials:

$$V(r)=A_{ij}\exp(-b_{ij}r)-C_{ij}/r^6 + q_iq_j/4\pi\varepsilon_0 r$$

Interaction	A_{ij} (eV)	b_{ij} (Å^{-1})	C_{ij} (eV Å^6)	Charge q
O–O	22 764.0	6.7114	27.88	$q_O = -2$
Ti–O	3 242.124	3.4626	0.0	$q_{Ti} = 4$
Ca–O	2 272.741	3.3490	0.0	$q_{Ca} = 2$

13

Profile of the primary order parameter (octahedra rotation) in $CaTiO_3$

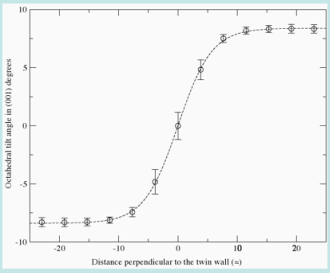

Profile of a secondary order parameter in $CaTiO_3$: Ti-Ti distances perpendicular to the wall. The wall is positioned at the origin

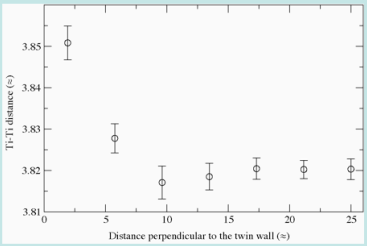

walls are elastically (a bit) softer

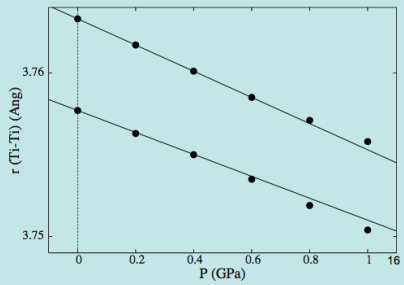

Relative change of the crystal total energy due to a single oxygen vacancy.

A twin wall along (100) with vanishing primary order parameter is at the origin. Circles denote vacancies for oxygen bridging Ti along [100], squares along [010] and diamonds along [001].

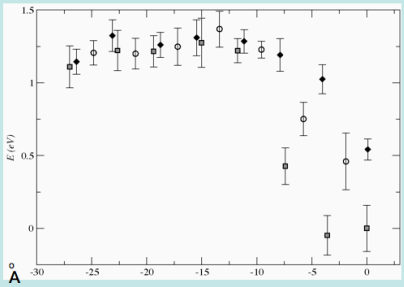

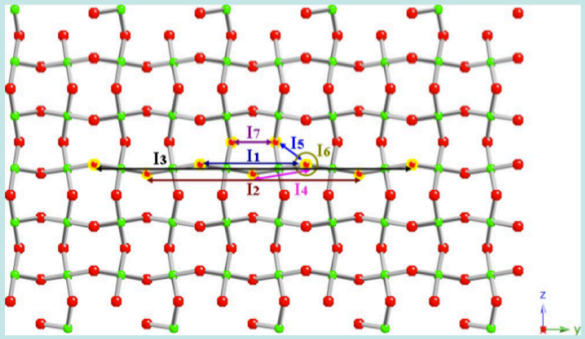

Correlation energy between vacancies are positive >> no clustering

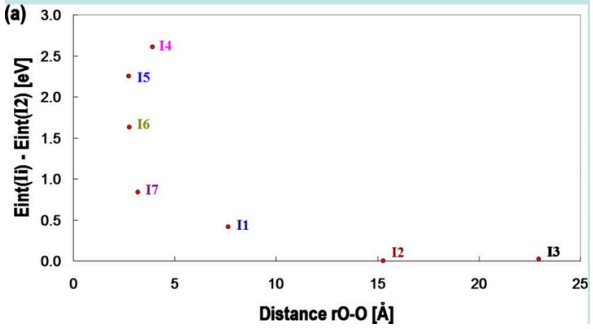

$CaTiO_3$: anti-ferroelectric Ti distortion in the x-z plane

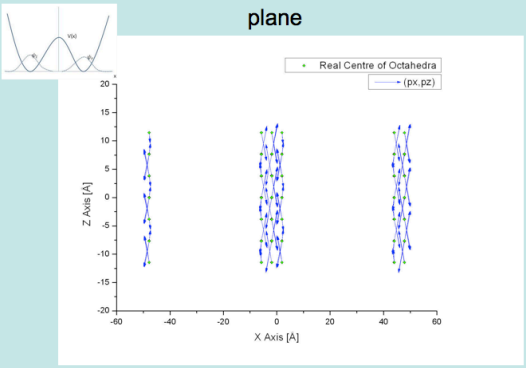

CaTiO3 ferroelectric and anti-ferroelectric distortion in ferroelastic twin walls

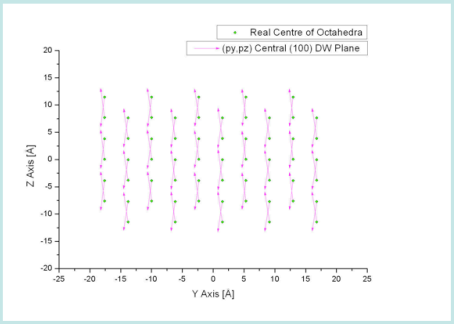

Surface structure often result from the incompatibility between bulk microstructures and surface relaxations (thin films)

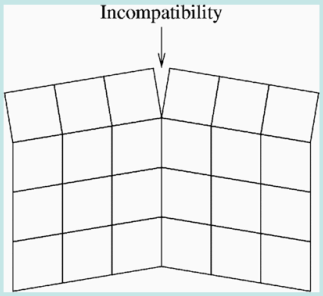

complex minimizer with 3 competing length scales: w, the surface relaxation and the exponential decay of the surface wave

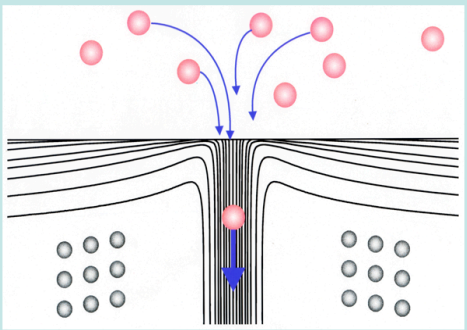

Salje and Conti, Novak and Salje, Conti et al (2010)

phase diagram for bi-quadratic coupling

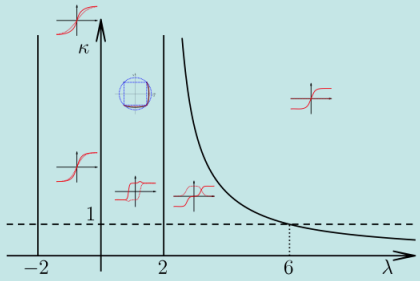

$F_\lambda(u,v)=(1-u^2)^2+(1-v^2)^2+\lambda u^2v^2-c\lambda$

$E_{\kappa,\lambda}[u,v]=\int F_\lambda(u,v)+|u'|^2+\kappa|v'|^2\,dx$

26

one kink (u) and one breather (v)

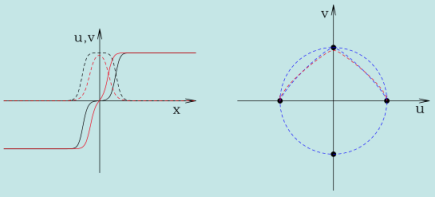

27

two breathers can increase the gradient in photovoltaics

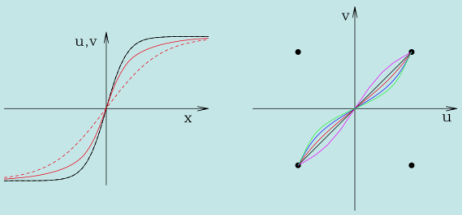

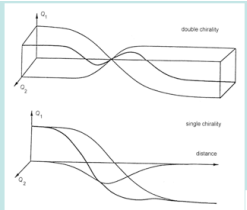

Two coupled order parameters

$G = \frac{1}{2} A_1 Q_1^2 + \frac{1}{4} B_1 Q_1^4 + \frac{1}{2} g_1 (Q'_1)^2 + \frac{1}{2} A_2 Q_2^2 + \frac{1}{4} B_2 Q_2^4 + \frac{1}{2} g_2 (Q'_2)^2 + \lambda Q_1^2 Q_2^2$

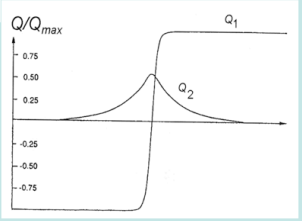

Linear-quadratic coupling

$G(Q,P) = \frac{1}{2}aQ^2 + \frac{1}{4}Q^4 + \frac{1}{2}cP^2 + \frac{1}{4}P^4 + \frac{1}{2}\lambda QP^2.$

$P^2 = -2a/\lambda\, Q - 2/\lambda\, Q^3$

$P^2 = -c - \lambda Q$

$Q^3 + (\lambda^2/2 + a)\, Q + c\lambda/2 = 0$

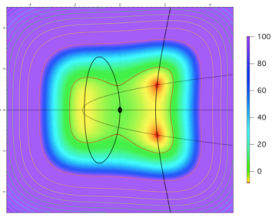

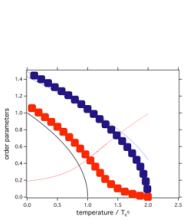

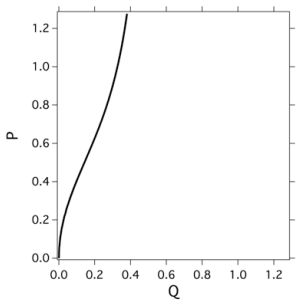

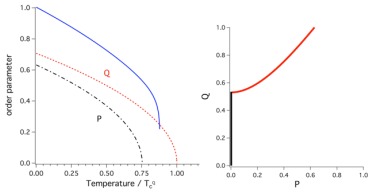

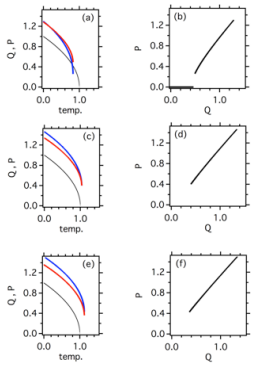

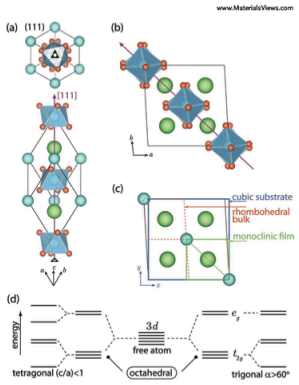

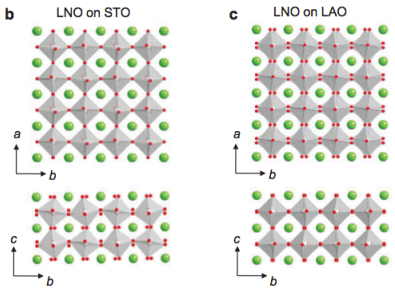

the next challenge: domain boundary engineering in thin films (here $LiNiO_3$ on $SrTiO_3$ and $LaAlO_3$)

dynamics of walls

ballistic (viscous),
accelerated,
jerky (avalanches)

36

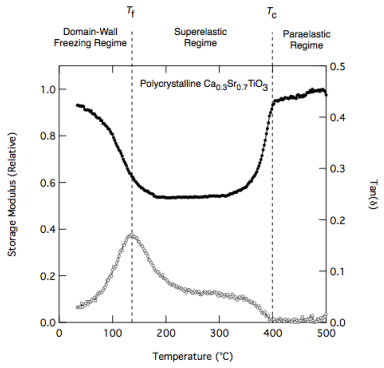

viscous motion:

extension of the Euler-Lagrange equation in d dimensions
using Landau-Khalatnikov

$\{ \partial^2/dr^2 + (d-1)/r\ \partial/\partial r - \tau/g\ \partial/\partial t \}\ Q = \{\partial/\partial Q\}\ G(Q)/g$

same profile , also in the ballistic limit with $\partial^2/\partial t^2$

leading to Lorentz contraction, for C=0
$Q(r,t) = Q_o \tanh\{ (r-vt)/(w[1-v^2/c^2]^{1/2})\}$
the wall profile does not change, only the wall thickness contracts
Pinning potential can be simulated atomistically and lead to very small pinning for thick walls (w>2 unit cells)

38

Frequency-dependence

90:100 mN

200:220 mN

450:500 mN

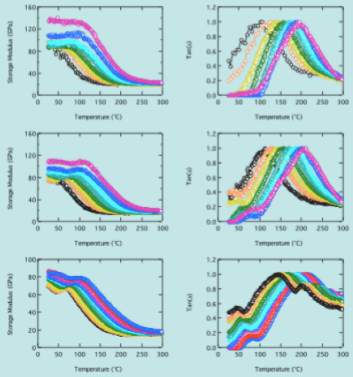

Elastic response function

- $J(t)=\varepsilon(t)/\sigma=J_{unrelaxed} + \Delta J(1-\exp(-t/\tau))$

$J(\omega)= J_{unrelaxed} + \Delta J\ (1/(1+i\omega\tau))$ Debye

- Extended Debye

$J(\omega)= J_{unrelaxed} + \Delta J\ (1/(1+i\omega\tau)^{\mu})$

- Equivalent to density function in τ

$\rho(\tau)=(\tau^{\mu-1}\sin(\mu\pi)/\pi)/(1+\tau^{2\mu}+2\tau^{\mu}\cos(\pi\mu))$

- First moment $\tau\rho(\tau)$ gives the probability function of τ

Elastic Cole-Cole plots: 'flattened' semicircles

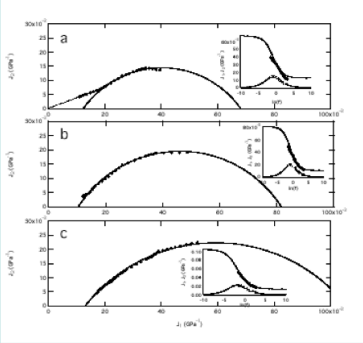

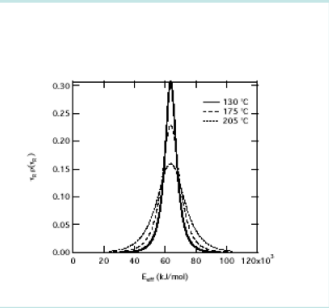

jerky movement: the noise of the propagating wall

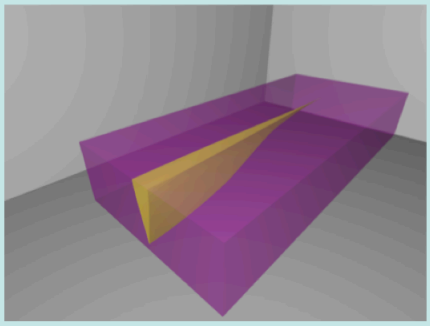

crumbling porous materials
fractal, also in magnetism

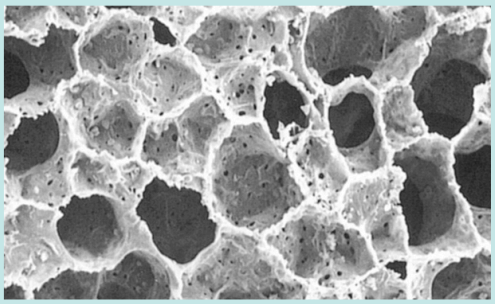

uniaxial stress

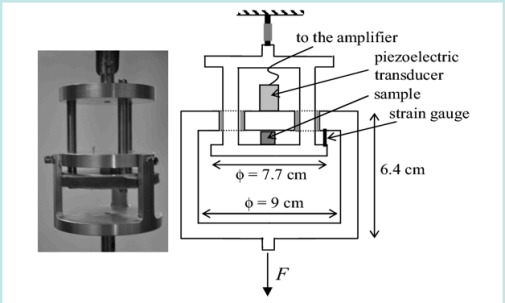

noise pattern

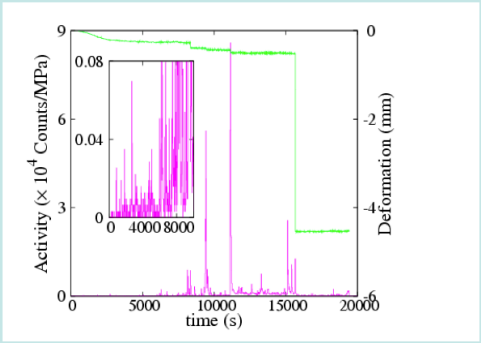

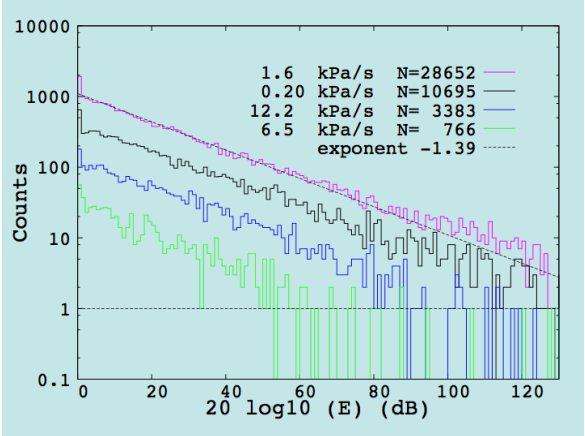

computer simulation: do jerks need defects? or can crystals crumble under elastic forces without being elastically unstable?

- the model: red and yellow lines are Landau springs

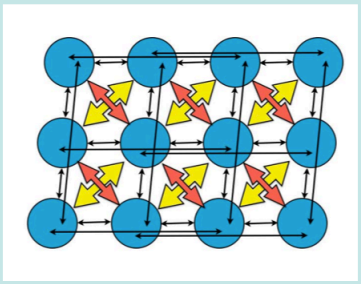

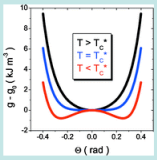

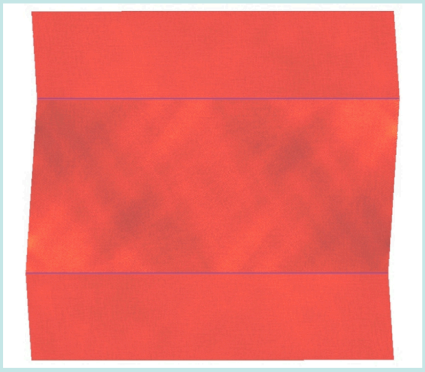

a defect free sample is sheared and jamms via twin boundaries

- notice the interplay between horizontal and vertical twin boundaries (Salje et al. PRB submitted)

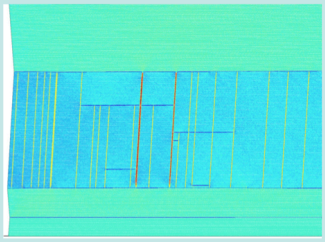

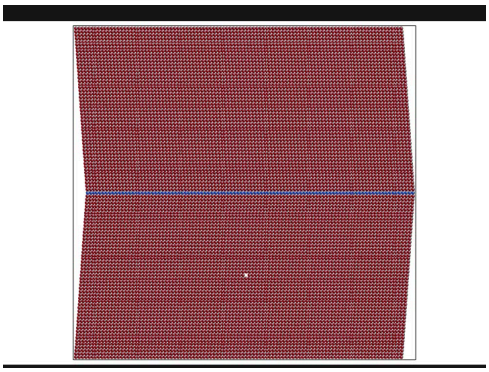

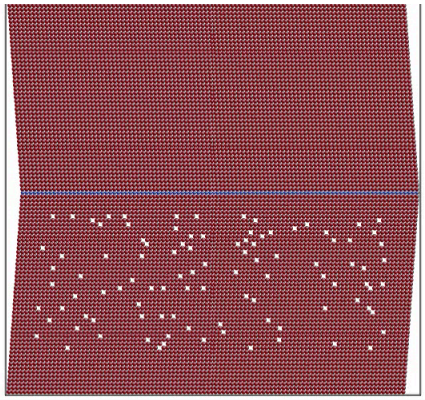

the response is sawtooth, the statistics is Vogel-Fulcher or power law

- high temperature lead
- to exponential decays with
- VF law while low temperatures
- leads to a-thermal power law

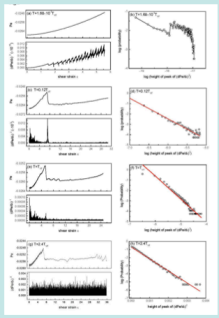

Inverse activation energy leads to VF law (regime III) with 'phase transition' to a power law regime (II) at the VF temperature. Regime (i) shows a purely mechanical response.